Eur. Phys. J. C 48, 787–796 (2006)
DOI 10.1140/epjc/s10052-006-0019-3

THE EUROPEAN PHYSICAL JOURNAL C

Regular Article – Experimental Physics

A Beta Beam complex based on the machine upgrades for the LHC

A. Donini[1], E. Fernandez-Martinez[1], P. Migliozzi[2,a], S. Rigolin[1], L. Scotto Lavina[3], T. Tabarelli de Fatis[4], F. Terranova[5]

[1] I.F.T. and Dep. Física Teórica, U.A.M., Madrid, Spain
[2] I.N.F.N., Sezione di Napoli, Naples, Italy
[3] Dip. di Fisica, Università "Federico II" and INFN, Napoli, Italy
[4] Universita di Milano Bicocca and I.N.F.N., Milano, Italy
[5] I.N.F.N., Laboratori Nazionali di Frascati, Frascati (Rome), Italy

Received: 3 May 2006 / Revised version: 12 July 2006 /
Published online: 24 October 2006 – © Springer-Verlag / Società Italiana di Fisica 2006

Abstract. The beta beam CERN design is based on the present LHC injection complex and its physics reach is mainly limited by the maximum rigidity of the SPS. In fact, some of the scenarios for the machine upgrades of the LHC, particularly the construction of a fast cycling 1 TeV injector ("Super-SPS"), are very synergic with the construction of a higher γ beta beam. At the energies that can be reached by this machine, we demonstrate that dense calorimeters can already be used for the detection of ν at the far location. Even at moderate masses (40 kton) as the ones imposed by the use of existing underground halls at Gran Sasso, the CP reach is very large for any value of θ_{13} that would provide evidence of ν_e appearance at T2K or NOνA ($\theta_{13} \geq 3^\circ$). Exploitation of matter effects at the CERN to Gran Sasso distance provides sensitivity to the neutrino mass hierarchy in significant areas of the $\theta_{13} - \delta$ plane.

PACS. 14.60.Pq; 14.60.Lm

1 Introduction

Since a few years, we have solid experimental evidence[1–6] that the ratio $\Delta m^2_{12}/|\Delta m^2_{23}|$ of the neutrino squared mass differences driving the solar and atmospheric oscillations is of the order of $\mathcal{O}(10^{-2})$. This measurement has an enormous impact in the design of future experiments posed to thoroughly determine the leptonic mixing matrix (PMNS [7,8]). In particular, given a relatively large $\Delta m^2_{12}/|\Delta m^2_{23}|$ ratio, the determination of the currently unknown 1–3 sector of the PMNS, i.e. the mixing between the first and third generation and the CP violating Dirac phase, can be accomplished by long baseline experiments measuring the contamination of $\nu_\mu \to \nu_e$ transitions in the bulk of $\nu_\mu \to \nu_\tau$ oscillations at the atmospheric scale. The size of these sub-dominant contributions depends on the mixing angle between the first and third neutrino generation (θ_{13}) and an experimental determination of this angle is mandatory to establish to what extent future facilities are able to address CP violation in the leptonic sector or fix the neutrino mass hierarchy (sign of Δm^2_{23}) exploiting matter effects. Should the size of θ_{13} be large enough to allow the observation of $\nu_\mu \to \nu_e$ oscillations at the atmospheric scale in the forthcoming experiments [9–17] ($\theta_{13} \gtrsim 3^\circ$), new facilities would be needed to close up the PMNS. They should perform precision measurements of the 1–3 sector and particularly of the CP violating phase. In this context a novel neutrino source like the beta beam [18] (BB) offers unprecedented opportunities thanks to the large intensities and purities available. Moreover, it represents a unique European facility since it could leverage the present CERN acceleration complex. Unfortunately, in its present design [19] the physics potential of the beta beam is not fully exploited [20–23]. The maximum rigidity of the CERN SPS machine limits the energy of the outgoing neutrinos, so that very large detectors are needed to overcome the smallness of the cross sections. Tuning the oscillation probability to the first peak, the corresponding baseline is too short to exploit matter effects and, hence, determine the sign of Δm^2_{23}. Moreover, dense detectors cannot be employed to separate ν_μ from ν_e interactions, so that enormous underground facilities must be built on purpose.

On the other hand, it is unlikely that the CERN acceleration complex will remain unchanged up to the time of operation considered in the baseline design (about 2020 [24]). In fact, some of the scenarios for the machine upgrades of the LHC are, accidentally, very synergic with a higher energy beta beam. In this paper, we identify the options that could leverage a strong neutrino programme aimed at a full

[a] e-mail: pasquale.migliozzi@cern.ch

determination of the PMNS and ν mass hierarchy, and the setups that can exploit existing underground facilities and moderately massive dense detectors (Sects. 2, 3 and 4). For any value of θ_{13} that allows evidence for $\nu_\mu \to \nu_e$ oscillations in the forthcoming experiments up to T2K [15, 16] or NOνA [17], we show that these setups have the sensitivity to address CP violation in the leptonic sector (Sect. 5). We also compute the minimum intensity required to guarantee full coverage of the T2K sensitivity region. We draw our conclusions in Sect. 6.

2 The accelerator complex

The steady progress in the technology of radioactive ion production and acceleration opens up the possibility of obtaining pure sources of ν_e directly from β unstable isotopes [18]. These sources have practically no contamination from other flavors and a well defined energy spectrum that depends on the kinematics of β decay. The choice of the isotope is a compromise between production yield, Q value and lifetime. Isotopes with short lifetimes, $\tau \lesssim 1$ s, must be handled by fast cycling boosters to avoid strong losses during the acceleration phase. On the other hand, larger lifetimes result in a decrease of the number of decays per unit time (hence, of ν flux) for a fixed number of ion stacked. The best isotopes identified so far are ^{6}He for antineutrino production (a β^- emitter with $E_0 = 3506.7$ keV and a 806.7 ms half life) and ^{18}Ne for neutrinos ($E_0 = 3423.7$ keV and half life of 1.672 s). The former is obtained by neutron absorption in beryllium oxide and requires a proton-to-neutron converter; the latter is produced through spallation, e.g. from proton interactions with a magnesium oxide target[1]. Both require a ~ 200 kW proton driver operating in the few GeV region. The collection and ionization of the ions is performed using the ECR technique. Hereafter ions are bunched, accelerated and injected up to the high energy boosters. In the baseline design, the proton driver is the proposed super proton linac (SPL) [27]. The SPL is a multi-megawatt (~ 4 MW, E_p =2.2 GeV [27] or 3.5 GeV [28, 29]) machine aimed at substituting the present Linac2 and PS booster (PSB). Contrary to naive expectation, a multi-megawatt booster is not necessary for the construction of a Beta Beam or a nuclear physics (EURISOL-like [30, 31]) facility and could be fully exploited only by a low-energy neutrino SuperBeam [32] or by a Neutrino Factory complex. Any of the possibilities currently under discussion at CERN [33, 34] for the upgrade of the PSB based either on Rapid Cycling Syncrotrons or on Linacs represents a viable solution for the production stage of a Beta Beam complex. They would allow production of $\sim 2 \times 10^{13}$ ^{6}He/s for 200 kW on target, consistently with the current SPL-based design. A proper upgrade of the sub-GeV boosters represents an important step toward full exploitation of the LHC physics capabilities; in particular, the luminosity of the large hadron collider would highly benefit from a modification of the pre-injectors, which are currently limited by space charge at the PSB and PS injection energies [35]. The choices and timescale for the upgrades of the LHC will depend on the feedbacks from the first years of data taking. Still, three phases can already be envisaged [35, 36]: an optimization of present hardware ("phase 0") to reach the ultimate luminosity of 2×10^{34} cm^{-2}s^{-1} at two interaction points; an upgrade of the LHC insertions ("phase 1") and, finally, a major hardware modification ("phase 2") to operate the LHC in the $\mathcal{L} \simeq 10^{35}$ cm^{-2}s^{-1} regime and, if needed, prepare for an energy upgrade. The most straightforward approach to "phase 2" would be the equipment of the SPS with fast cycling superconducting magnets in order to inject protons into the LHC with energies of about 1 TeV. At fixed apertures at injection, this option would double the peak luminosity of the LHC. Moreover, injecting at 1 TeV strongly reduces the dynamic effects of persistent currents, ease stable operation of the machine and, therefore, impact on the integrated luminosity of the collider. The 1 TeV injection option ("Super-SPS") would have an enormous impact on the design of a Beta Beam at CERN. This machine fulfills simultaneously the two most relevant requirements for a high energy BB booster: it provides a fast ramp ($\mathrm{d}B/\mathrm{d}t = 1.2 \div 1.5$ T/s [37]) to minimize the number of decays during the acceleration phase and, as noted in the first Reference of [20–23], it is able to bring ^{6}He up to $\gamma \simeq 350$ (^{18}Ne to $\gamma \simeq 580$). In this case, neutrinos are produced by the beta beam with energies of the order of few GeV ($\langle E \rangle = 2.18$ GeV for neutrinos, 1.35 for antineutrinos). As shown in Sect. 4, this energy allows the use of dense detectors and existing underground infrastructures, the first peak of oscillation probability being comparable to the CERN to Gran Sasso distance. Due to the large increase of the cross-section, a strong reduction of the detector mass is possible compared with the baseline design. Clearly, the exploitation of the Super-SPS as a final booster for the BB is not in conflict with LHC operations, since the Super-SPS operates as injector only for a small fraction of its duty time (LHC filling phase).

The use of the Super-SPS as the final booster of the BB is not the only possibility that can be envisaged to reach the multi-GeV regime. After injection of the ions from the SPS to the LHC, a mini-ramp of the LHC itself would bring the ions at $\gamma = 350$–580. Differently from the previous case, however, this option would require allocation of a significant fraction of the LHC duty cycle for neutrino physics and could be in conflict with ordinary collider operations. Moreover, this option requires dedicated machine studies to quantify the injection losses or optimize the dipole ramp. For these reasons, in the following we mainly focus on the exploitation of the Super-SPS[2].

The increase of the ion energy in the last element of the booster chain represents a challenge for stacking [39]. Ions

[1] Recently a novel method to produce high intensity (^{8}Li and ^{8}B) beams has been put forward in [25]. Using these beams interesting physics results can be obtained [26].

[2] It is worth mentioning that the Super-SPS eases substantially injection of β-unstable ions in the LHC to reach $\gamma \gg 350$–580. For a discussion of this option we refer to [38].

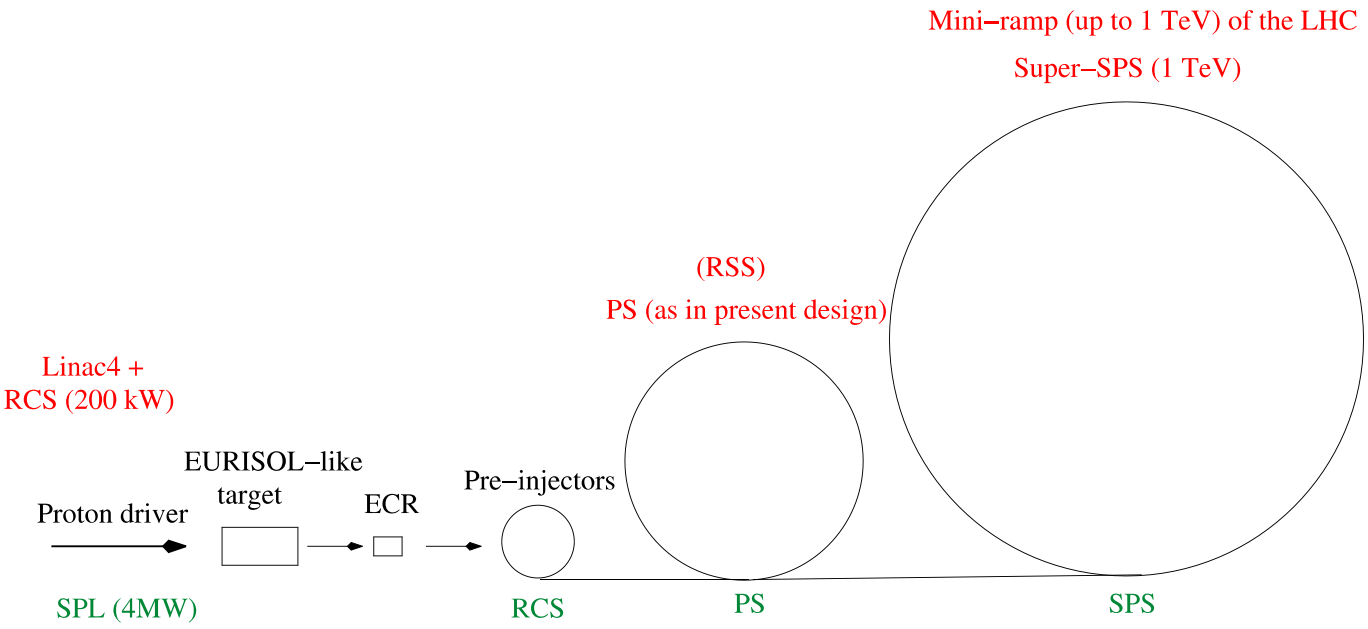

Fig. 1. The main components of the beta beam complex up to injection into the decay ring. In the *lower part*, the machines considered in the baseline option are indicated. The alternatives that profit of the upgrade of the LHC injection system are also mentioned (*upper part*). RCS stands for rapid cycling syncrotron, RSS for rapid superconducting syncrotron [34]. Other abbreviations are defined in the text

of high rigidity must be collected in a dedicated ring of reasonable size. In the baseline design, this is achieved by a decay ring made of small curved sections (radius $R \sim 300$ m) followed by long straight sections ($L = 2500$ m) pointing toward the far neutrino detector. In this case, the decays that provide useful neutrinos are the ones occurring in the straight secsion where neutrinos fly in the direction of the detector and the useful fraction of decays ("livetime") is limited by the decays in the opposite arm of the tunnel. For the CERN to Frejus design the livetime is $L/(2\pi R + 2L) \sim 36\%$ and the overall length has been fixed to 6880 m. A decay ring of the same length equipped with LHC dipolar magnets (8.3 T) would stack ions at the nominal Super-SPS rigidity with a significantly larger radius (~ 600 m). The corresponding livetime is thus 23%. Again, current R&D related with the LHC upgrades and aimed at the development of high field magnets ($11 \div 15$ T) [35, 40] can be used to reduce the costs for the decay ring and increase the livetime[3]. An additional reduction of flux comes from the increase of ion lifetime (about a factor of three for ^{6}He at $\gamma = 350$ compared with the baseline option at $\gamma = 100$ [41]). There is, however, a strong correlation between the increase of the neutrino energy and the amount of ions that can be stacked into the decay ring. In the baseline design, the constraint on the number of circulating bunches and on the bunch length comes from the need of timing the parent ion. This is mandatory to suppress the atmospheric background in the far detector. The smaller the time occupancy of the ion bunches in the ring, the larger the suppression factor (SF):

$$\mathrm{SF} = \frac{\Delta t_\mathrm{b} \cdot N_\mathrm{b} \cdot v}{2\pi R + 2L} \qquad (1)$$

Δt_b being the time length of the bunch, N_b the number of circulating bunches, $v \simeq c$ the ion velocity and $2\pi R + 2L$ the length of the ring. In the baseline design this value must be kept at the level of 10^{-3}, implying a challenging $\Delta t_\mathrm{b} = 10$ ns time structure of the bunch for $N_\mathrm{b} = 8$ circulating bunches. At higher energies (e.g. $\gamma = 350$ for ^{6}He) the atmospheric background is suppressed by about one order of magnitude and the SF can be correspondingly relaxed, provided that the injection system can sustain the increased request of bunches and/or ions per bunch. Since a complete machine study concerning this issue is still missing[4] – especially for the Super-SPS – in the following, physics performances are determined as a function of fluxes. We remind that the baseline BB design aims at 2.9×10^{18} ^{6}He and 1.1×10^{18} ^{18}Ne decays per year ("nominal intensity"). Figure 1 sketches the main components of the BB complex up to injection into the decay ring. In the lower part, the machines considered in the baseline option are listed. The alternatives that profit of the upgrade of the LHC injection system are also mentioned (upper part).

[3] The correspondence between the various magnet R&D and the BB is not accidental: in a BB complex the booster plays the role of the collider injector and, hence, profits of the requirements for fast cycling; the decay ring plays the role of the collider, which is aimed at the highest possible rigidity, even at the expense of the ramp time. Clearly, ramping speed is immaterial for the BB stacking ring.

[4] For recent progresses in the framework of the baseline design (SPS-based), see [42].

3 Far detector concept and expected rates

Traditional technologies for ν production (up to the so-called "Superbeams") allow the investigation of the 1–3 sector of the leptonic mixing matrix through the appearance of ν_e and $\bar{\nu}_e$ at baselines ≥ 100 km, i.e. through the information coded in the $\nu_\mu \to \nu_e$ and $\bar{\nu}_\mu \to \bar{\nu}_e$ transitions probabilities. In this context, optimal far detectors are low-density, massive e.m. calorimeters (liquid scintillators, water Cherenkov, liquid Argon TPC's [43]). On the other hand, both the beta beams and the Neutrino Factories [44, 45] exploit the T-conjugate channel $\nu_e \to \nu_\mu$ and $\bar{\nu}_e \to \bar{\nu}_\mu$. In the case of the beta beam, oscillated neutrinos are the *only* source of primary muons while for the neutrino factory the detector must be able to identify the muon charge with outstanding efficiencies ($> 99.9\%$) to distinguish the $\nu_e \to \nu_\mu$ signal from the $\bar{\nu}_\mu$ background. In both cases, calorimetric measurements are needed to reconstruct the neutrino energy[5]. In particular, the choice of the passive material of the calorimeter depends on the typical range of the primary muon; the latter must be significantly larger than the interaction length to allow for filtering of the hadronic part and effective NC and ν_e CC selection. For neutrinos of energies greater than ~ 1 GeV, iron offers the desired properties. As a consequence, the energy of the Super-SPS can be exploited to switch from a low-Z to a high-Z/high-density calorimeter also in the case of the beta beam. The use of iron detectors avoids the need for large underground excavations, which are mandatory for beta beams at lower ν energies. Since these detectors are capable of calorimetric measurements, they can be exploited even better than water Cherenkov to obtain spectral informations. They're not expected to reach, anyhow, the granularity of liquid argon TPC's or the megaton-scale mass of water Cherenkov's; hence, in spite of the underground location, they cannot be used for proton decay measurements and low-energy astroparticle physics.

Magnetization of the iron is not strictly necessary, even if it contributes to reducing the pion punch-through background (the sign of the primary muon is uniquely determined by the ion species circulating in the stacking ring). Since the neutrino energy at the Super-SPS matches the CERN to Gran Sasso baseline, a high density calorimeter can be hosted into the existing halls of the Gran Sasso laboratories up to fiducial masses of ~ 40 kton.

Figure 2 shows the corresponding neutrino fluxes (nominal intensity) at the Gran Sasso location for both ^{6}He and ^{18}Ne at $\gamma = 350$ ("$\gamma = 350, 350$ option") and for ^{18}Ne at the Super-SPS maximum rigidity ($\gamma = 580$: "$\gamma = 350, 580$ option"). The calculation include the effects of finite electron mass and the three different decay modes of ^{18}Ne, each with a different end-point energy, see Table 1.

A relevant source of uncertainty in the determination of the event rates is the present poor knowledge of the νN and $\bar{\nu} N$ cross-sections for energies below 1 GeV [49]: either there are very few data (the case of neutrinos) or there are no data at all (the case of antineutrinos). On top of that, the few available data have generally not been taken on the target used in the experiments (either water, iron, lead or plastics), and the extrapolation from different nuclei is non trivial. The situation improves at the energies relevant for the Super-SPS although this region is still below the DIS dominated regime. Note, moreover, that a much improved knowledge of the cross sections will be available in the forthcoming years both due to a dedicated experimental campaigns [50] and from the near detectors of the next generation long baseline experiments.

We use in this paper the cross-section on iron obtained following [51, 52]. In Table 2 the expected unoscillated ν_e CC events per kton-year are shown for $\gamma = 350, 580$ together with the fraction of QE, RES and DIS in the sample.

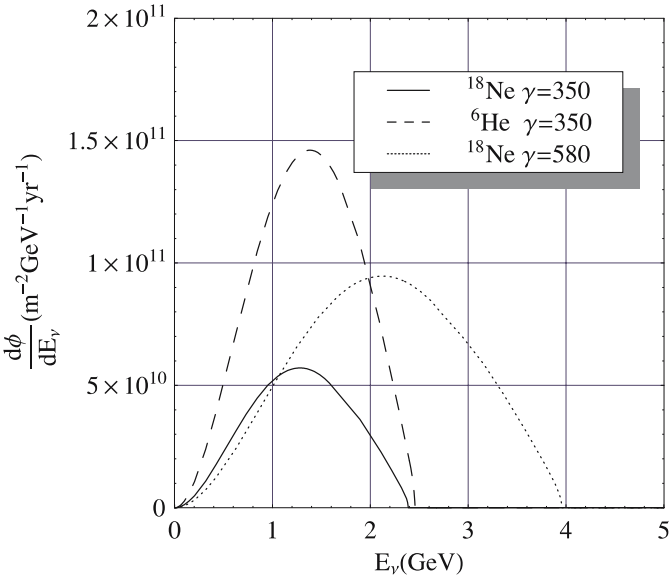

Fig. 2. Beta Beam fluxes at the Gran Sasso location (735 km baseline) as a function of the neutrino energy

Table 1. ^{18}Ne and ^{6}He β-decay channels and relative end-point energies from [48]

Element	End-point (MeV)	Decay fraction
^{18}Ne	34.114	92.1%
	23.699	7.7%
	17.106	0.2%
^{6}He	35.078	100%

Table 2. Expected unoscillated ν_e CC events per kton-year

	ν (350)	ν (580)	$\bar{\nu}$ (350)
DIS	1.57	75.18	0.06
RES	16.76	60.82	29.72
QE	37.47	115.37	30.28
Total	55.80	251.36	60.7

[5] The only notable exception concerns the "monochromatic beta beams"[46, 47] based on ions decaying through electron capture.

4 The iron calorimeter

Several techniques can be employed for the design of the active detectors of large mass iron calorimeters. Due to cost constraints, most of the options are based on plastic scintillators or gaseous detectors. In the present study, we consider a design derived from a digital hadron calorimeter proposed for the reconstruction of the energy flow at the ILC detector [53–55] and based on glass resistive plate chambers (DHCAL). In this case, gas detectors are particularly appealing since they allow highly granular designs. On the other hand, in the context of the beta beam the advantages mainly reside on the low production cost of RPC, along the line investigated by the MONOLITH [56] and INO [57] collaborations. Clearly, a systematic comparison of the options available is beyond the scope of the present work.

The configuration considered hereafter consists of a sandwich of 4 cm non-magnetized iron interleaved with glass RPC's to reach an overall mass of 40 kton. The RPC are housed in a 2 cm gap; the active element is a 2 mm gas-filled gap; the drift field is produced by 2 mm thick glass electrodes coated with high resistivity graphite. The signal is readout on external pick-up electrodes segmented in $2 \times 2\,\mathrm{cm}^2$ pads, providing a single-bit information. A full GEANT3 [58] simulation of this geometry has been implemented along the lines discussed in [54, 55], including a coarse description of the RPC materials and an approximate description of the digitization process. Spark generation in the active medium is assumed to happen with 95% efficiency upon the passage of an ionising particle. As detailed in [54, 55], the accuracy of this simulation has been validated by comparing its predictions to existing data collected with a small prototype exposed to a pion beam of energy from 2 GeV to 10 GeV [59]. Inclusive variables (total number of hits and event length expressed in terms of number of crossed iron layers) have been used for event classification[6]. The scatter plot of the event length versus the total number of hits of the event is shown in Fig. 3 for neutrinos (left panel) and anti-neutrinos (right panel) both coming from ions accelerated at $\gamma = 350$. ν_μ and ν_e charged-current (CC) interactions as well as neutrino neutral-current (NC) interactions are shown with different colors. An interaction is classified as a ν_μ CC-like event if both the event length and the total number of hits in the detector are larger than 12. In the case the ^{18}Ne is ran at $\gamma = 580$, we classify an event as a CC-like interaction if the event length and the total number of hits are larger than 15 and 17, respectively. The typical efficiency for identifying a neutrino or anti-neutrino CC interaction averaged out over the whole spectrum is of the order of 50%–60%. Conversely, the probability for the background to be identified as a CC-like event is slightly less than 1%. Compared with more challenging beta beams or neutrino factory designs, this facility offers a limited pion rejection capability; this is due to the low energy of the neutrinos (compared with the neutrino factory or very high gamma beta beam options) and the choice of a dense detector. Still, as we demonstrate in the subsequent sections, these performances are sufficient to explore CP violation in the leptonic sector for any value of θ_{13} that gives a positive ν_e appearance signal in

[6] The event discrimination capability can be further improved developing a dedicated pattern recognition system aimed at identifying explicitly hits belonging to the primary muons.

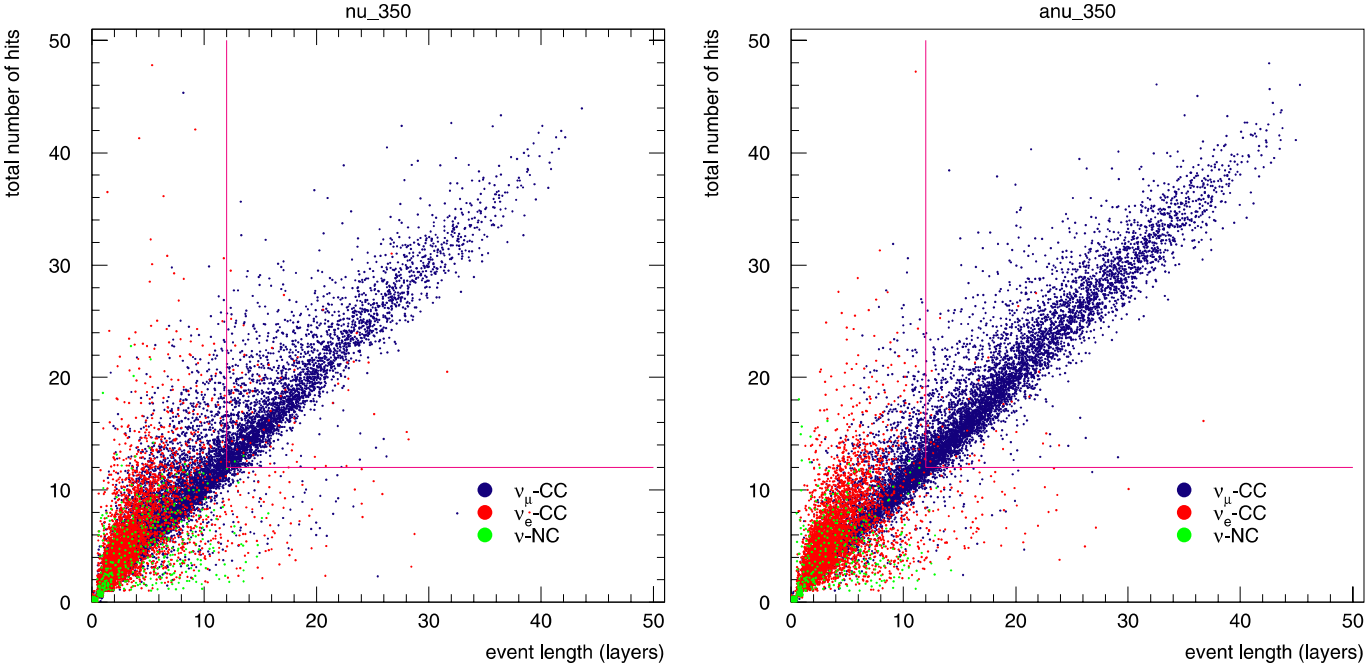

Fig. 3. Scatter plot of the total number of hits recorded in the detector versus the total length (given in number of crossed layers) of the event for neutrinos (*left*) and anti-neutrinos (*right*) with $\gamma = 350$

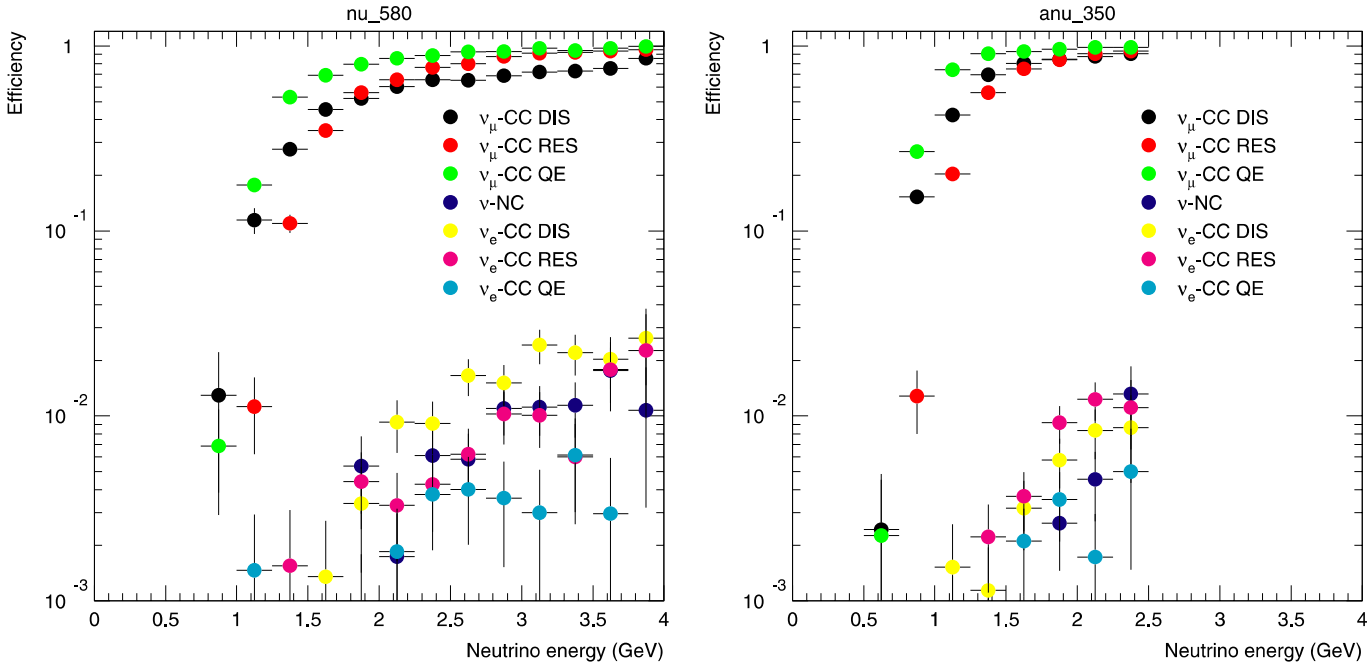

Fig. 4. Efficiencies for the signal (ν_μ and $\bar{\nu}_\mu$ charged-current interactions) to be identified as CC-like event and for the background (ν_e and $\bar{\nu}_e$ interactions, and ν_μ and $\bar{\nu}_\mu$ neutral-current interactions) to be mis-identified as a CC-like events

the next generation of long-baseline experiments: MINOS, OPERA and the so-called "Phase I" experiments based on Superbeams (T2K, NOνA) or reactors.

Finally, the efficiencies to correctly identify ν_μ and $\bar{\nu}_\mu$ charge-current interactions are shown for deep-inelastic (DIS), quasi-elastic (QE) and resonance (RES) production, separately, in Fig. 4 as well as the probability that ν_e and $\bar{\nu}_e$, separately for DIS, QE and RES production, and neutral-current interactions are identified as a CC-like interaction.

5 Evaluation of the physics reach

The currently unknown mixing parameters θ_{13} and δ determine the inclusive rate of ν_μ (N^-) and $\bar{\nu}_\mu$ (N^+) CC events at the far location. Matter effects, moreover, are sizable at baselines comparable to the CERN to Gran Sasso distance and introduce additional modifications. In particular, for positive (negative) mass hierarchy and positive (negative) values of the Dirac CP phase, it is possible to determine the sign of Δm^2_{23} from the simultaneous measurements of N^+ and N^-. Matter effects induce also spectral distortions in the ν_μ and $\bar{\nu}_\mu$ distributions that improve the sensitivity and help in the ambiguous region of negative (positive) CP phases. In the following, sensitivities are computed from a binned likelihood fit of the N^+ and N^- samples. The likelihood incorporates the finite energy resolution of the detector (migration matrices) computed from the full simulation of Sect. 4. Atmospheric background is neglected together with the systematics affecting the $\nu/\bar{\nu}$ ratio and a 2% systematic uncertainty in the detector efficiency is assumed.

The expected number of events as a function of δ and θ_{13} are shown in Table 3 for nominal fluxes. For the already measured oscillation parameters, we assumed the following values: $\Delta m^2_{12} = 8.2 \times 10^{-5}\,\mathrm{eV}^2$; $\theta_{12} = 33^\circ$; $\Delta m^2_{23} = 2.5 \times 10^{-3}\,\mathrm{eV}^2$ [60]. In the rest of this paper we only consider positive Δm^2_{23} and $\theta_{23} = 45^\circ$, in this way only the intrinsic degeneracy is accounted for.

5.1 Establishing CP violation in the leptonic sector

The main task of the second generation of accelerator experiments (beyond T2K or NOνA) is the search for an additional source of CP violation in the universe coming from three-family leptonic mixing. As noted above, significant constraints on the size of δ can be put only if θ_{13} is not highly suppressed. The next generation of long baseline and reactor experiments is designed to explore θ_{13} regions down to $\sim 3^\circ$ and a positive result will likely trigger the construction of "Phase II" facilities as the one discussed in this paper. Therefore, it is of paramount importance to test down to what δ value CP violation can be established for *any* value of θ_{13} that can be accessed by T2K or NOνA. For the present facility, this is shown in Fig. 5 as a function of the flux (F_0 corresponds to nominal fluxes for ^{6}He and ^{18}Ne). In particular, the horizontal bands indicate the regions excluded at 90% CL by T2K [7]. Clearly, even at fluxes

[7] Exclusion limits depends significantly on the true (unknown) value of δ, especially if no antineutrino run is foreseen [61]. In the plot, limits at $\delta = 90^\circ, 0^\circ, -90^\circ$ are indicated.

Table 3. Event rates for a 10 years exposure. The observed oscillated CC events for different values of δ and θ_{13} are given assuming normal neutrino mass hierarchy and $\theta_{23} = 45^\circ$. The expected background is also reported

θ_{13}	δ	ν_μ CC $\gamma = 350$	ν_μ CC $\gamma = 580$	$\bar{\nu}_\mu$ CC	ν-back $\gamma = 350$	ν-back $\gamma = 580$	$\bar{\nu}$-back
1°	-90°	1.43	9.44	37.33	126.02	881.11	77.28
5°	-90°	105.44	485.48	266.89	126.02	881.11	77.28
10°	-90°	541.17	2291.01	848.62	126.02	881.11	77.28
1°	0°	18.27	80.45	22.58	126.02	881.11	77.28
5°	0°	189.51	840.07	193.23	126.02	881.11	77.28
10°	0°	708.67	2997.51	701.85	126.02	881.11	77.28
1°	90°	32.23	99.40	2.61	126.02	881.11	77.28
5°	90°	259.27	934.72	93.49	126.02	881.11	77.28
10°	90°	847.67	3186.08	503.13	126.02	881.11	77.28

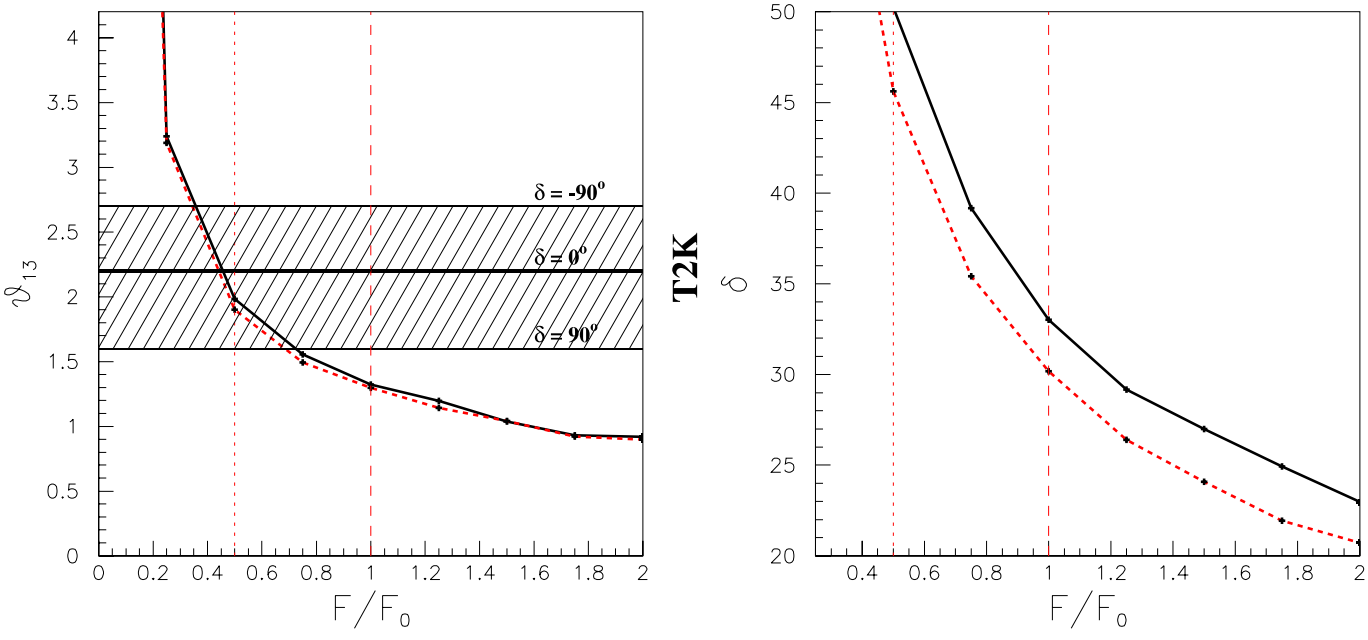

Fig. 5. *Left plot*: minimum θ_{13} where CP violation can be established at 99% C.L. for $\delta = 90^\circ$ as a function of the flux (1 corresponds to F_0). *Right plot*: minimum δ that can be distinguished from zero, at 99% C.L., as a function of the neutrino flux for $\theta_{13} = 3^\circ$. *Black (dark) line* corresponds to the $\gamma = 350, 350$ option, *red (light)* to the $\gamma = 350, 580$ option

significantly smaller than F_0, maximal ($\delta = 90^\circ$) CP violation can be established. For values of $\theta_{13} = 3^\circ$ (where T2K has reasonable chance to report solid evidence of ν_e appearance for a wide range of δ values) this beta beam facility operated at nominal fluxes can establish CP violation (at 99% CL) down to $\delta \sim 30^\circ$ (see Fig. 5 right plot). The minimum δ_{CP} that can give evidence of CPV at 99% C.L., as a function of θ_{13}, is shown in Fig. 6 for various fluxes. To ease comparison with current literature, the discovery potential of the SPS-based beta beam with a Mton-size water Cherenkov detector ("baseline option") is also reported[8] [62, 63].

In case of null result[9] additional constraints can be put in the $\theta_{13} - \delta$ parameter phase. They are shown in Fig. 7 together with the limits from the baseline beta beam option.

5.2 Neutrino hierarchy

As noted above, matter effects perturb the transition probabilities and a simultaneous fit of the energy distributions for neutrinos and antineutrinos allows to fix the neutrino hierarchy (sign of Δm^2_{23}) in large areas of the $\theta_{13} - \delta$ plane.

[8] For a comparison with water Cherenkov detectors operated at high γ beta beams see [20–23].

[9] This implies the possibility of a second generation facility to be built independently from the outcome of T2K, NOνA and the novel reactor experiments.

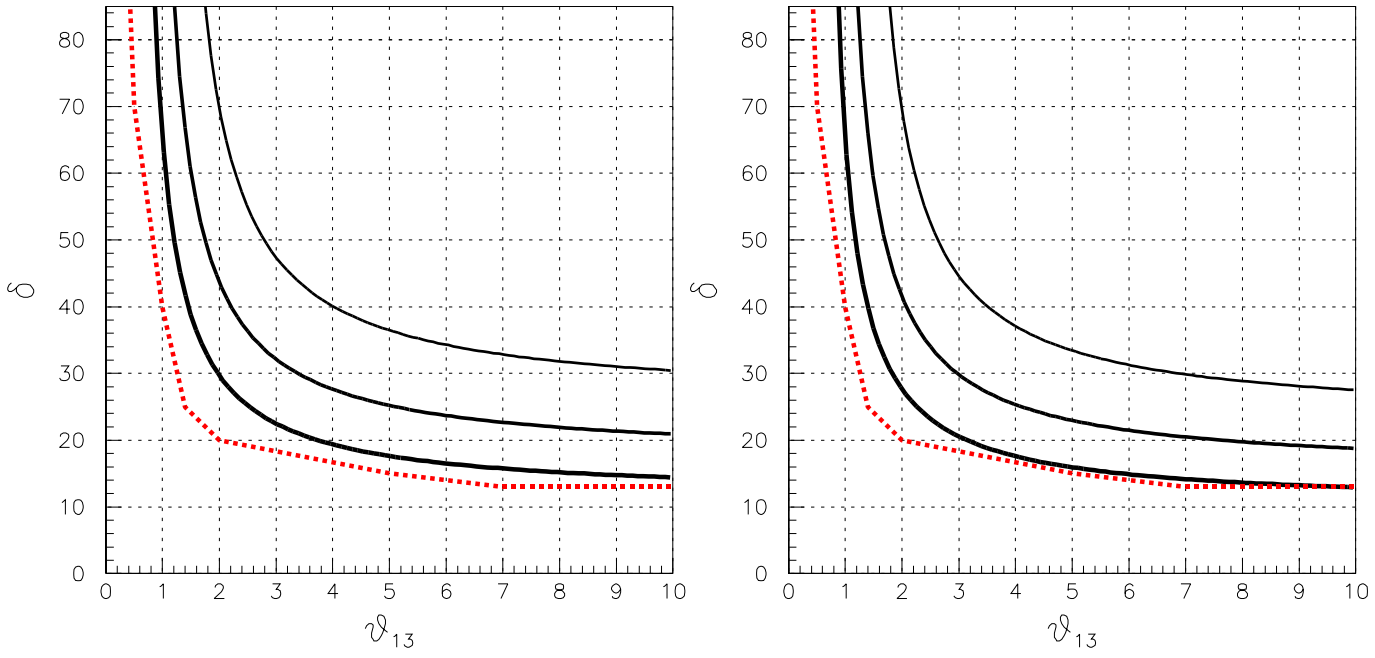

Fig. 6. $\delta_{\rm CP}$ discovery potential at 99% C.L. as a function of θ_{13} for the $\gamma = 350, 350$ (*left plot*) and $\gamma = 350, 580$ (*right plot*) option. The different *solid lines* corresponds to different fluxes. From left to right: $2\times F_0$, F_0 and $F_0/2$. The *dashed line* show the discovery potential for the baseline beta beam option as computed in [62]

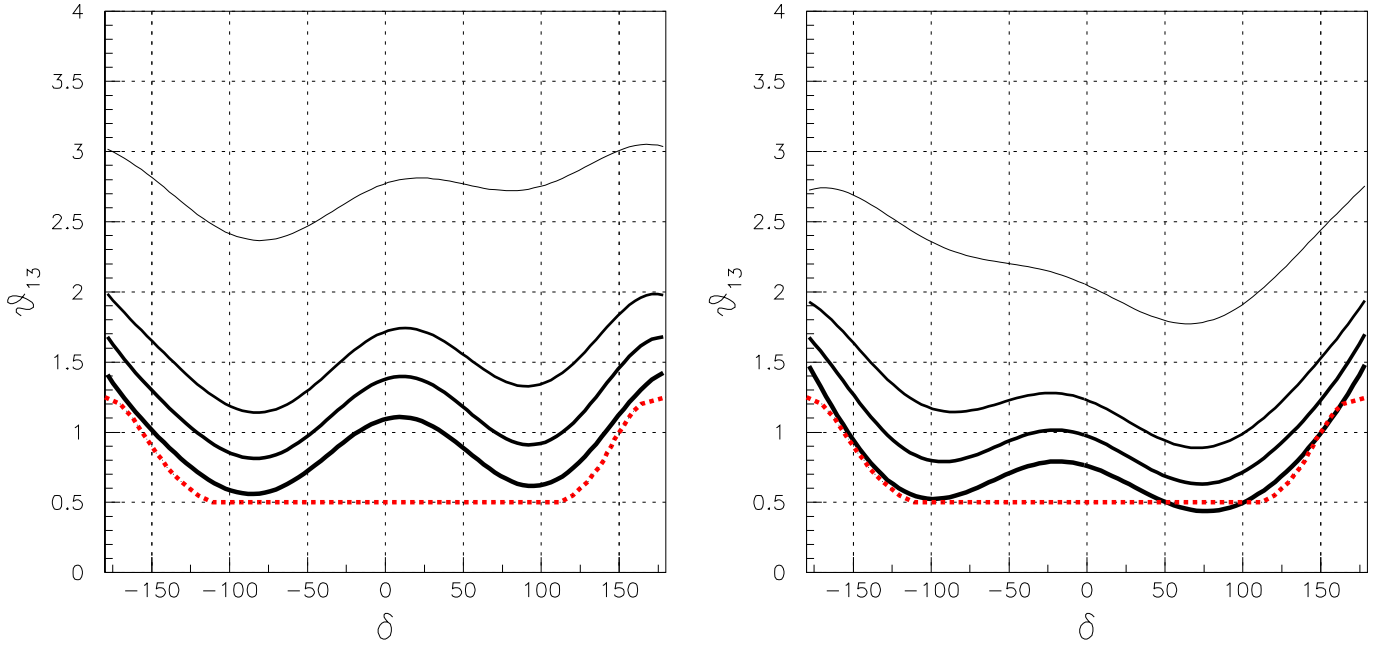

Fig. 7. θ_{13} limits at 90% C.L. as a function of δ for the $\gamma = 350, 350$ (*left plot*) and $\gamma = 350, 580$ (*right plot*) option. The different *solid lines* corresponds to different fluxes. From down to top: $2\times F_0$, F_0, $F_0/2$ and $F_0/10$. The *dashed line* show the limits for the baseline scenario as computed in [62]

Figure 8 shows the $\theta_{13} - \delta$ region where the sign of Δm^2_{23} can be established to be positive at 99% C.L. (normal hierarchy; the plot for inverted hierarchy is almost symmetric with respect to the $\delta = 0$ axis). As already discussed, for $\Delta m^2_{23} > 0$ ($\Delta m^2_{23} < 0$) the sensitivity mainly resides in regions of positive (negative) δ.

6 Conclusions

It is an established fact that the physics case for a CERN-based Beta Beam is limited by the smallness of the outgoing neutrino energy. The CERN design is based on the present LHC injection complex and it is limited by the

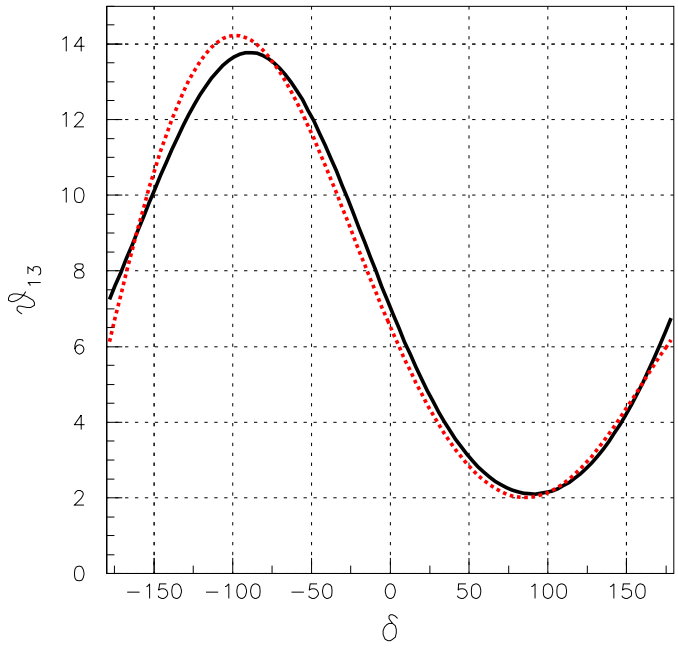

Fig. 8. Region of the parameter space where it is possible to distinguish at 99%C.L. the (true) hypothesis $\Delta m^2_{23} > 0$ from the $\Delta m^2_{23} < 0$. *Black (dark) line* corresponds to the $\gamma = 350, 350$ option, *red (light)* to the $\gamma = 350, 580$ option

rigidity of the SPS and the intensity that can be handled at PS. On the other hand, removal of these constraints is highly beneficial to the LHC itself. In particular, the construction of a fast cycling 1 TeV machine ("Super-SPS") as the one proposed in the context of the "Phase II" lumi upgrade of the LHC can improve substantially the physics reach of the european beta beam. In this paper, we discussed in detail the synergies between the LHC machine upgrades and the beta beam technology. At the energies that can be reached by the Super-SPS, we demonstrated that dense detectors (iron calorimeters) can already be used. Even at moderate masses (40 kton) as the one imposed by the use of existing underground halls at Gran Sasso, the CP reach is very large for any value of θ_{13} that would provide evidence of ν_e appearance at T2K or NOνA. Moreover, exploitation of matter effects (impossible with SPS-based options) add sensitivity to the neutrino hierarchy. Therefore, the beta beam represents a very relevant enhancement of the case for a fast cycling 1 TeV injector at CERN.

Acknowledgements. We wish to express our gratitude to F. Ferroni, M. Lindroos, M. Mezzetto, F. Ronga and W. Scandale for many useful discussions.

References

1. SNO Collaboration, Q.R. Ahmad et al., Phys. Rev. Lett. **87**, 071 301 (2001)
2. SNO Collaboration, B. Aharmim et al., arXiv:nucl-ex/0502021
3. KamLAND Collaboration, T. Araki et al., Phys. Rev. Lett. **94**, 081 801 (2005)
4. Super-Kamiokande Collaboration, Y. Ashie et al., arXiv:hep-ex/0501064
5. MACRO Collaboration, M. Ambrosio et al., Phys. Lett. B **566**, 35 (2003)
6. K2K Collaboration, E. Aliu et al., Phys. Rev. Lett. **94**, 081 802 (2005)
7. B. Pontecorvo, Sov. Phys. JETP **6**, 429 (1957)
8. Z. Maki, M. Nakagawa, S. Sakata, Prog. Theor. Phys. **28**, 870 (1962)
9. MINOS Collaboration, M.A. Thomson et al., Nucl. Phys. Proc. Suppl. **143**, 249 (2005)
10. ICARUS Collaboration, F. Arneodo et al., ICARUS-TM/2001-08 LNGS-EXP 13/89 add.2/01
11. OPERA Collaboration, M. Guler et al., CERN-SPSC-2000-028
12. M. Komatsu, P. Migliozzi, F. Terranova, J. Phys. G **29**, 443 (2003)
13. Double Chooz Collaboration, F. Ardellier et al., arXiv:hep-ex/0405032
14. K. Anderson et al., arXiv:hep-ex/0402041
15. T2K Collaboration, Y. Itow et al., arXiv:hep-ex/0106019
16. T2K Collaboration, Y. Hayato et al., Nucl. Phys. Proc. Suppl. **143**, 269 (2005)
17. NOvA Collaboration, D.S. Ayres et al., arXiv:hep-ex/0503053
18. P. Zucchelli, Phys. Lett. B **532**, 166 (2002)
19. J. Bouchez, M. Lindroos, M. Mezzetto, AIP Conf. Proc. **721**, 37 (2004)
20. J. Burguet-Castell, D. Casper, J.J. Gomez-Cadenas, P. Hernandez, F. Sanchez, Nucl. Phys. B **695**, 217 (2004)
21. A. Donini, E. Fernandez-Martinez, P. Migliozzi, S. Rigolin, L. Scotto Lavina, Nucl. Phys. B **710**, 402 (2005) [arXiv:hep-ph/0406132]
22. A. Donini, E. Fernandez-Martinez, S. Rigolin, Phys. Lett. B **621**, 276 (2005) [arXiv:hep-ph/0411402]
23. J. Burguet-Castell, D. Casper, E. Couce, J.J. Gomez-Cadenas, P. Hernandez, Nucl. Phys. B **725**, 306 (2005) [arXiv:hep-ph/0503021]
24. J. Bouchet, talk at the Workshop on the Next Generation of Nucleon Decay and Neutrino Detectors (NNN05), 7–9 April 2005, Aussois, France
25. C. Rubbia, A. Ferrari, Y. Kadi, V. Vlachoudis, arXiv:hep-ph/0602032
26. A. Donini, E. Fernandez-Martinez, arXiv:hep-ph/0603261
27. B. Autin et al., Conceptual design of the SPL, a high-power superconducting H^- linac at CERN, CERN-2000-012
28. R. Garoby, The SPL at CERN, CERN-AB-2005-007, contribution to the 33rd ICFA Advanced Beam Dynamics Workshop: High Intensity High Brightness Hadron Beams (ICFA HB2004), Bensheim, Germany, 2004
29. J.E. Campagne, A. Cazes, Eur. Phys. J. C **45**, 643 (2006)
30. Workshop on Radioactive beams for nuclear physics and neutrino physics, 37th Rencontre de Moriond, Les Arcs (France) March 17–22nd, 2003
31. http://moriond.in2p3.fr/radio/index.html
32. M. Mezzetto, J. Phys. G **29**, 1781 (2003)
33. J.B. Dainton et al., Fixed-Target Physics at CERN beyond 2005 Summary and Conclusions of an Evaluation by the SPSC (Villars meeting 22-28 September 2004), CERN-SPSC-2005-010, 2005
34. R. Garoby, W. Scandale, Nucl. Phys. Proc. Suppl. **147**, 16

(2005)
35. O. Bruning et al., LHC luminosity and energy upgrade: A feasibility study, CERN-LHC-PROJECT-REPORT-626, 2002
36. W. Scandale, High Intensity Injection Chain for LHC, talk at the High Intensity Frontier Workshop (HIF05), La Biodola, Italy, 2005
37. P. Fabbricatore, Rapid Cycling SC Magnets, ibid
38. F. Terranova, A. Marotta, P. Migliozzi, M. Spinetti, Eur. Phys. J. C **38**, 69 (2004)
39. F. Terranova, Nucl. Phys. Proc. Suppl. **149**, 185 (2005)
40. A. Devred et al., Status of the Next European Dipole (NED) activity of the Collaborated Accelerator Research in Europe (CARE) project, CERN-AT-2005-002
41. M. Lindroos, talk at the Workshop on the Next Generation of Nucleon Decay and Neutrino Detectors (NNN05), 7–9 April 2005, Aussois, France
42. M. Lindroos, EURISOL DS/TASK12/TN-05-02
43. A. Guglielmi, M. Mezzetto, P. Migliozzi, F. Terranova, arXiv:hep-ph/0508034
44. S. Geer, Phys. Rev. D **57**, 6989 (1998) [Erratum-ibid. D **59**, 039 903 (1999)]
45. A. De Rujula, M.B. Gavela, P. Hernandez, Nucl. Phys. B **547**, 21 (1999)
46. J. Bernabeu, J. Burguet-Castell, C. Espinoza, M. Lindroos, JHEP **0512**, 014 (2005)
47. J. Sato, Phys. Rev. Lett. **95**, 131 804 (2005)
48. L.P. Ekström, R.B. Firestone, WWW Table of Radioactive Isotopes, from http://ie.lbl.gov/toi/index.htm
49. G.P. Zeller, arXiv:hep-ex/0312061
50. G.P. Zeller, Nucl. Phys. Proc. Suppl. **155**, 111 (2006) [arXiv:hep-ex/0603001]
51. P. Lipari, private communication
52. P. Lipari, M. Lusignoli, F. Sartogo, Phys. Rev. Lett. **74**, 4384 (1995)
53. G. Alexander et al., TESLA Technical Design Report. Part. IV: A Detector for TESLA, ed. by T. Behnke, S. Bertolucci, R.D. Heuer, R. Settles, DESY-01-011, DESY-2001-011, DESY-01-011D, DESY-2001-011D, DESY-TESLA-2001-23, DESY-TESLA-FEL-2001-05, ECFA-2001-209
54. A. Ghezzi, T. Tabarelli de Fatis, G. Tinti, M. Piccolo, Digital hadron calorimetry with glass RPC active detectors, Contributed to 2005 International Linear Collider Workshop (LCWS 2005), Stanford, California, 18–22 Mar 2005
55. arXiv:physics/0507021
56. MONOLITH Collaboration, N.Y. Agafonova et al., MONOLITH: A massive magnetized iron detector for neutrino oscillation studies, LNGS-P26-2000, CERN-SPSC-2000-031, CERN-SPSC-M-657
57. G. Rajasekaran, AIP Conf. Proc. **721**, 243 (2004)
58. GEANT – Detector Description and Simulation Tool CERN Program Library Long Writeup W5013
59. M. Ambrosio et al., Nucl. Instrum. Methods A **456**, 67 (2000)
60. M.C. Gonzalez-Garcia, arXiv:hep-ph/0410030
61. P. Migliozzi, F. Terranova, Phys. Lett. B **563**, 73 (2003)
62. M. Mezzetto, Nucl. Phys. Proc. Suppl. **155**, 214 (2006) [arXiv:hep-ex/0511005]
63. J.E. Campagne, M. Maltoni, M. Mezzetto, T. Schwetz, arXiv:hep-ph/0603172